In situ high-pressure study of diborane by infrared spectroscopy

Yang Song,[1,a)] Chitra Murli,[1] and Zhenxian Liu[2]
[1]*Department of Chemistry, The University of Western Ontario, London, Ontario N6A 5B7, Canada*
[2]*Geophysical Laboratory, Carnegie Institution of Washington, Washington, D.C. 20015, USA*

(Received 16 August 2009; accepted 6 October 2009; published online 3 November 2009)

As the simplest stable boron hydride in its condensed phase, diborane exhibits an interesting structural chemistry with uniquely bridged hydrogen bonds. Here we report the first room-temperature infrared (IR) absorption spectra of solid diborane compressed to pressures as high as 50 GPa using a diamond anvil cell. At room temperature and 3.5 GPa, the IR spectrum of diborane displays rich sharply resolved fundamentals and overtones of the IR active bands, consistent with the previous low-temperature IR measurements of condensed diborane at ambient pressure. When compressed stepwise to 50 GPa, several structural transformations can be identified at pressures of ~3.5 GPa, ~6.9 GPa and ~14.7 GPa, as indicated by the changes in the band profile as well as the pressure dependence of the characteristic IR modes and bandwidths. These transformations can be interpreted as being enhanced intermolecular interactions resulting from compression. The geometry of the four-member ring of B_2H_6, however, does not seem to be altered significantly during the transformations and the B_2H_6 molecule remains chemically stable up to 50 GPa. © *2009 American Institute of Physics*. [doi:10.1063/1.3257627]

I. INTRODUCTION

Diborane (B_2H_6) has an interesting ring-type molecular structure with peculiar bridged hydrogen bonds. Due to the extremely reactive nature of single borane (BH_3) which rapidly dimerizes into stable B_2H_6, diborane thus represents the simplest stable boron hydride. Although kinetically stable, diborane is an endothermic compound (ΔH_f= +36 kJ mol^{-1})[1] and thus has been used as a versatile reagent in a large number of industrial and laboratory applications.[2] The reactivity of diborane is largely associated with hydrogen loss, which makes this material a promising lightweight hydrogen storage material with 22 wt % hydrogen, among the candidates with the highest hydrogen content for hydrogen storage. Its higher hydride form, pentaborane (B_5H_9), has already been investigated as a possible hydrogen-based fuel for high-speed jets. In addition, it has been documented that diborane can undergo polymerization into higher boron hydrides,[3] which makes borane chemistry an intriguing area for both experimental and theoretical studies.

The molecular, electronic, and crystal structures as well as the special hydrogen bridge bonding of diborane have all been extensively characterized by various approaches, including electron diffractions,[4] x-ray diffraction,[5,6] and vibrational spectroscopy,[7–11] as well as several theoretical studies.[3,12–15] In addition to the ambient pressure studies, Barbee III *et al.*[16] investigated the structures and stabilities of boron hydrides at elevated pressures by computational methods. Stable molecular boranes at ambient pressure were found to become unstable such that new structures with extended networks characterized by covalent or even metallic bonding interactions may be formed. The significance of the new boranes formed at high pressures is that these energetic structures may be suitable as hydrogen storage media if they are metastable and thus recoverable on the release of pressure. Experimentally, Nakano *et al.*[17] reported high pressure studies of decaborane ($B_{10}H_{14}$) using Raman, IR, and visible transmission spectroscopy. A nonmolecular phase with a loss of covalent B–H bonding was found to form above 100 GPa. Inspired by the results of these studies, we here report the first high-pressure IR spectroscopic study of diborane compressed in a diamond anvil cell up to 50 GPa. At ambient pressure and below 60 K, solid diborane crystallizes into the α phase with an orthorhombic structure (a=7.89, b=4.54, and c=6.89 Å, Z=4), while annealing to above 90 K results in the formation of β phase (space group $P2_1/n$, a=4.40, b=5.72, and c=6.50 Å, and γ=105.1°).[5,6] However, high-pressure structures and stabilities of diborane at room temperature remain completely unknown. Using *in situ* synchrotron infrared (IR) absorption spectroscopy, we observed several pressure-induced structural transformations. Our results thus make a significant contribution to the understanding of the high-pressure structures of diborane.

II. EXPERIMENTAL

Electronic grade gaseous diborane (purity 99.99%) packed in a lecture bottle with a 10% concentration balanced with hydrogen was purchased from Sigma-Aldrich and used without further purification. Loading was done by precooling a diamond anvil cell in liquid nitrogen. Because the melting point for B_2H_6 is −165 °C, gaseous B_2H_6 solidified on the cooled rhenium gasket of the cell in a liquid nitrogen bath. The cells were then sealed and the solid B_2H_6 was pressurized before warming to room temperature. A few ruby chips were inserted to facilitate pressure measurements before the

[a)]Author to whom correspondence should be addressed. Electronic mail: yang.song@uwo.ca. Tel.: (519)661-2111. Ext. 86310. FAX: (519)661-3022.

cryogenic loading. The pressure was determined from the well established pressure shift of the R_1 ruby fluorescence line with an accuracy of ± 0.05 GPa under quasihydrostatic conditions.[18] For the entire pressure region, ruby fluorescence spectra obtained on different ruby chips across the sample chamber indicated that there was no significant pressure gradient, indicating that B_2H_6 itself is an excellent pressure transmitting media in the pressure regions examined in the current study.

IR experiments were performed at the U2A beamline at the National Synchrotron Light Source (NSLS) at Brookhaven National Laboratory (BNL). The IR beam from the storage ring was extracted through a wedged diamond window from a source at a 40×40 mrad^2 solid angle and was collimated to a 1.5 in. diameter beam before entering a Bruker IFS 66V vacuum FT-IR spectrometer in conjunction with three microscope systems. The spectrometer was equipped with a number of beam splitters and detectors including a silicon bolometer and a mercury cadmium telluride (MCT). For mid-IR measurements, the IR beam was focused on the sample using a Bruker IR microscope and then the spectrum was collected in transmission mode by the MCT detector in the 600–8000 cm^{-1} spectral range. A resolution of 4 cm^{-1} was used in all IR measurements. For IR measurements, a sample thickness of 35 μm was used to allow sufficient IR transmission measurements. For all measurements, mid-IR spectra were collected through a 30×30 μm^2 aperture. The reference spectrum, i.e., the diamond anvil absorption at ambient pressure, was later divided as background from each sample spectrum to obtain the absorbance.

III. RESULTS AND DISCUSSION

A. IR spectrum of B_2H_6 at 3.5 GPa and room temperature

The IR absorption spectrum of diborane collected at 3.5 GPa (the lowest pressure point upon loading in the present study) is depicted in Fig. 1 as compared to those reported in the gas phase and in 2,3-diemthylbutane solution,[19] both at room temperature. The normal mode assignments are performed based on the comparison with previous low-temperature IR measurements and are listed in Table I. The diborane molecule maintains a D_{2h} symmetry in both the gas and crystalline phases, and thus the irreducible representation for molecular B_2H_6 is

$$\Gamma_{D_{2h}}(B_2H_6) = 4A_g + 2B_{1g} + 2B_{2g} + 1B_{3g} + 1A_u + 2B_{1u} + 3B_{2u} + 3B_{3u},$$

where all the ungerade modes are IR active except for A_u. Although the factor group of the B_2H_6 crystal lattice may predict a multiple of the above fundamentals and the symmetry of the normal modes may differ from D_{2h}, the IR bands can still be identified based on the D_{2h} molecular symmetry even in the condensed phase. As can be seen, all predicted IR active modes are observed, except for the ν_1 (B_{2u}) mode associated with the molecular ring puckering, which was predicted to occur at a much lower frequency (i.e., 379 cm^{-1}) than the spectral range of our study. In addition, rich combinations and overtones of fundamentals were also observed. The bands at 1070, 1412, and 1782 cm^{-1} are likely the combinations involving the ν_{14}, ν_{18}, and ν_{17} fundamentals and a lattice mode, respectively. At frequencies higher than 2300 cm^{-1}, except for the ν_{16} and ν_8 fundamentals at 2570 and 2630 cm^{-1}, which are, respectively, associated with terminal BH symmetric and antisymmetric stretch, all bands are combinations or overtones. The assignments of these bands are based on the close proximity to a combination of the fundamental frequencies where at least one intense fundamental, such as ν_{14}, ν_{18}, and ν_{17} modes, participates in the combination. However, the assignment of all combinations should still be considered tentative. As compared to the gas-phase IR spectrum of B_2H_6, all bands are characterized by sharper profiles, especially for the ν_{16} and ν_8 modes which are completely resolved in both the solution phase and the present high-pressure phase. The spectrum we collected at 3.5 GPa and at room temperature is also roughly consistent with those spectra measured at low temperatures in the condensed phase reported by Freund (Fig. 4 of Ref. 10). The difference in the band profile and the different combination bands are likely associated with the temperature factor.

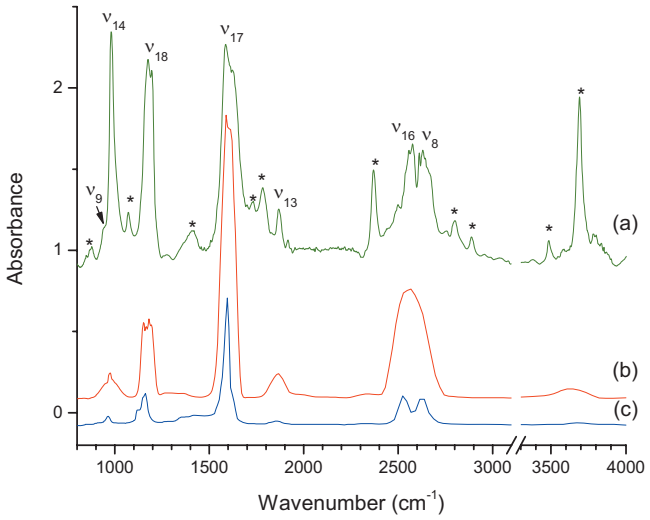

FIG. 1. IR absorption spectrum of B_2H_6 collected at 3.5 GPa and at room temperature (a) in comparison with previous measurements (from Ref. 19) taken in the gaseous phase (b) and in a 2,3-diemthylbutane solution (c). The spectra are vertically offset for clarity. The assignments for fundamentals are labeled above the present spectrum while those for combinations and overtones are labeled with asterisks (see text and Table I).

B. IR spectrum of B_2H_6 on compression

Starting from 3.5 GPa, we compressed B_2H_6 to around 50 GPa stepwise and observed several structural transformations. The absorption spectra as a function of pressure in the mid-IR spectral region of 800–4600 cm^{-1} are depicted in Fig. 2. As shown, when pressure was elevated to 5.4 GPa, several noticeable changes took place. A small but broad band at 872 cm^{-1}, which was most probably a combination of lattice modes, developed into one that was much sharper, similar to the evolution of another combination band (i.e., ν_{18}+lattice) at 1412 cm^{-1}. In contrast, the intensity of the band at 1070 cm^{-1} was markedly reduced. In addition,

TABLE I. Observed IR modes of diborane with assignments compared to previous IR measurements.

Symmetry	Mode	Duncan[a] (1981)	Freund[b] (1965)	This study[c]	Description[d,e]
B_{2u}	ν_8	2608	2597	2630	BH (t) antisymm. stretch
	ν_9	938	934	944	BH(t) in phase rock
	ν_{10}	379	···	···	Ring puckering
B_{1u}	ν_{13}	1884	1879	1870	BH (b) stretch/ring def.
	ν_{14}	970	966	980	BH(t) in phase wag
B_{3u}	ν_{16}	2512	2511	2570	BH(t) sym stretch
	ν_{17}	1586	1587	1608	BH (b) stretch/ring def.
	ν_{18}	1162	1161	1176	BH (t) antisymm. def.
Combinations/overtones				1070	ν_{14}+lattice
			1375	1412	ν_{18}+lattice
			···	1782	ν_{17}+lattice
			2319	2371	$2\nu_{18}$
			···	2800	$\nu_{17}+\nu_{18}$
			···	2888	$\nu_{13}+\nu_{14}$
			···	3485	$\nu_{13}+\nu_{17}$
			···	3689	$\nu_8+\nu_{14}$
				4164[f]	$\nu_{16}+\nu_{17}$

[a]Reference 11. The measurements were obtained from polycrystalline films at 60–78 K.
[b]Reference 10. The measurements were obtained from polycrystalline solid at −190 °C.
[c]Measured at room temperature and 3.5 GPa.
[d]Reference 12.
[e]The vibrations involving the B–H bond were labeled with t (terminal) or b (bridge) depending on the location of the B–H in the B_2H_6 molecule.
[f]Observed starting from 5.4 GPa.

the intense ν_{14} mode exhibited a slight splitting at 5.4 GPa. The most dramatic changes occurred in the high frequency region above 2300 cm^{-1}. Two new bands at 2511 and 4164 cm^{-1} can be observed, which can be assigned as combination bands. Furthermore, the ν_8 fundamental band and a combination band ($\nu_{13}+\nu_{17}$) at 3485 cm^{-1} were substantially depleted when compressed to 5.4 GPa. Concurrently, the physical appearance of the transparent sample under an optical microscope was found to change markedly indicating a change in the refraction index. These spectroscopic and optical observations suggest that B_2H_6 underwent a possible phase transition from liquid to solid. Far-IR measurements would be helpful to corroborate such a transition.

Continuing compression to above 6.9 GPa results in another series of changes in the IR spectra. Both the sharp low-frequency mode at 872 cm^{-1} and the band at 2511 cm^{-1} developed at 5.4 GPa, together with two high-frequency combination bands (i.e., $\nu_{17}+\nu_{18}$ and $\nu_{13}+\nu_{14}$) are almost completely depleted. In contrast, the depleted combination band at 1020 cm^{-1} is recovered at 9.9 GPa. In addition, a shoulder band of the ν_{18} mode at 1236 cm^{-1} starts to evolve, in contrast with the combination band of ν_{17} +lattice and the ν_{13} fundamental, which merged into a broad band at 9.9 GPa. These observations collectively suggest that there is yet another structural transformation above 6.9 GPa.

The next transition of B_2H_6 can be identified when the sample is compressed above 14.7 GPa. The band profiles of all the fundamental and combination modes exhibit a prominent broadening, especially for the ν_{14}, ν_{18}, and ν_{17} modes. The band broadening is accompanied by the development of an asymmetric profile of ν_{14} mode and an enhanced splitting of the ν_{18} mode. The merged band involving the ν_{13} fundamental at 9.9 GPa completely disappeared above 14.7 GPa. The most remarkable change is the observation of a new mode at 2760 cm^{-1}, a frequency close to the ν_8 fundamental that was otherwise not present in the spectra at 5.4 to 14.7 GPa. The ν_8 mode is characterized by the antisymmetric stretch of a terminal BH bond. The disappearance and reappearance of this mode suggest that the local environment was changed significantly by compression and that the antisymmetric stretch motion is extremely sensitive to compression. Beyond 16.7 GPa, all of the IR bands evolve with pressure smoothly and very gradually. Noticeable changes include the significant broadening of the ν_{14} and ν_{17} fundamentals and the combination band of $\nu_8+\nu_{14}$, further splitting of the ν_{18} mode, and the gradual diminishing of the overtone of $2\nu_{18}$ and ν_8 fundamental mode. No further dramatic changes were observed up to 50 GPa, indicating a single phase in this pressure region.

C. Discussion

In order to better understand the overall pressure-induced structural transformations, we plotted the frequencies of the major IR bands as a function of pressure as shown in Fig. 3. In addition, the full width at half maximum (FWHM) of two fundamentals, i.e, ν_{14} and ν_{17} modes, were also analyzed as a function of pressure and plotted as shown in Fig. 4. As can be seen, the frequencies of all IR modes blueshift with increasing pressure, consistent with the enhanced stiffness of all the B–H bonds upon compression. However, a change in the shift rate in different pressure re-

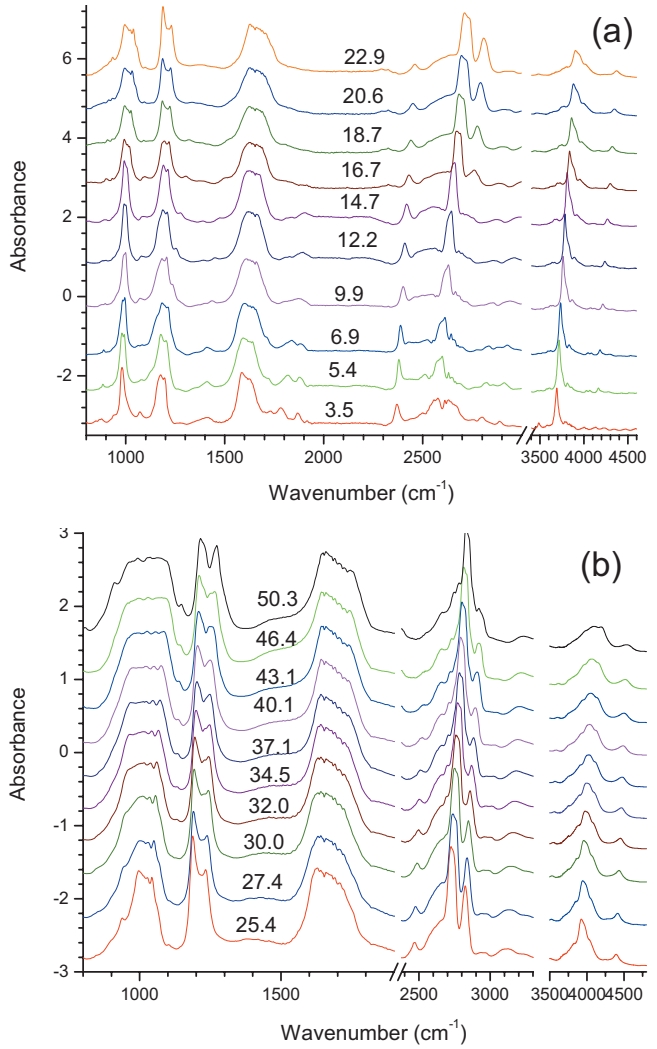

FIG. 2. IR absorption spectra of B_2H_6 collected upon compression from (a) 3.5 to 22.9 GPa and (b) 25.4 to 50.3 GPa in the spectral region of 800–4600 cm^{-1}. The spectra are vertically offset for clarity. The pressures in GPa are labeled above each spectrum. The spectral region of 3000–3400 cm^{-1} in (a) and that of 3300–3500 cm^{-1} in (b) are truncated due to the lack of spectroscopic features while that of 1900–2400 cm^{-1} has been omitted due to interference from the diamond absorption at higher pressures.

gions provides additional evidence of possible phase transitions. In the region below 6.9 GPa, almost all modes shift to higher frequencies more quickly (i.e., have a steeper pressure slope) than those in the subsequent higher pressure regions, indicating a higher compressibility in the low pressure region. It is well known that materials in the liquid phase or the low-density solid phase are typically more compressible than those in the high-density phases. The significantly different number of IR bands and the different pressure dependences of the bandwidth of the ν_{14} and ν_{17} modes (Fig. 4) observed below and above 6.9 GPa indicate a phase boundary around this pressure. The phase between 6.9 and 14.7 GPa likely has a different crystal structure and extent of ordering of the B_2H_6 molecules than the lower-pressure solid phase evidenced by the different IR signatures and bandwidths. The constant bandwidths with a plateau region between 6.9 and 16.7 GPa (Fig. 4) suggest that the material maintains good crystallinity and molecular ordering under compression.

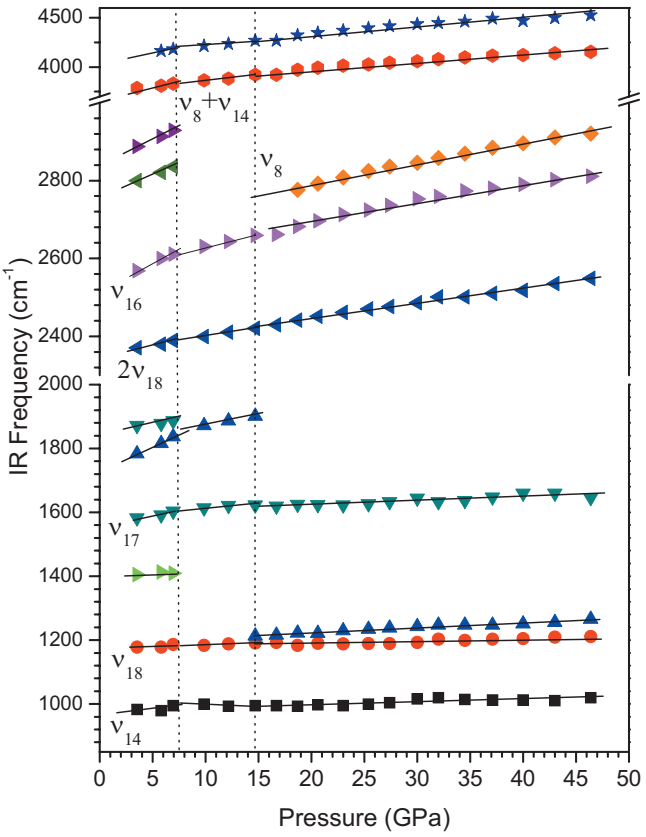

FIG. 3. Pressure dependence of the IR frequencies of the fundamentals and selected combination modes of B_2H_6 on compression. Different symbols denote different IR origins with assignments labeled on the left hand side. The vertical dashed lines indicate the proposed phase boundaries.

B_2H_6 appears to be structurally stable with no significant change in compressibility in this pressure region.

Beyond 14.9 GPa, the emergence of a new mode close to the ν_8 mode as well as the splitting of the ν_{18} mode are

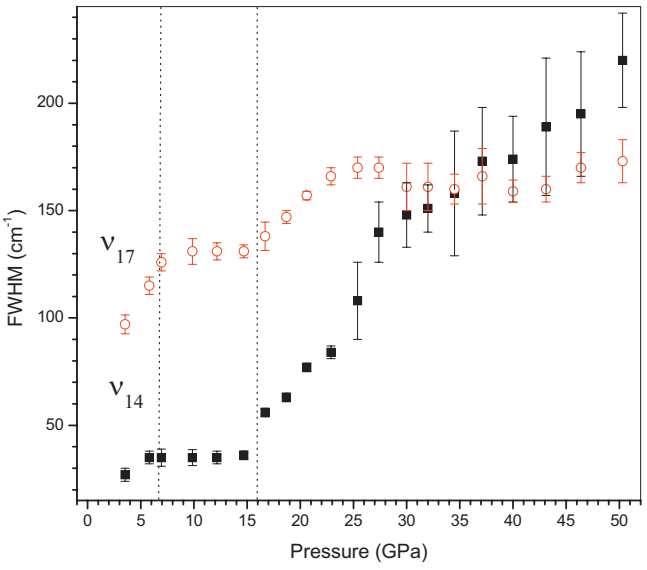

FIG. 4. FWHM of the ν_{14} mode (solid square) and ν_{17} mode (open circles) as a function of pressure from 3.5 to 50.3 GPa. Error bars are indicated for some pressures where the least squares fitting of the band profile carries larger uncertainties than average. The vertical dashed lines indicate the proposed phase boundaries.

probably due to the substantial changes in the intermolecular interactions via the terminal B–H groups resulting in a possible structural rearrangement, since both modes involve terminal B–H vibrations. The significant broadening of all IR bands, especially in the ν_{14} mode (Fig. 4), whose bandwidth increased more than six times from 14.9 to 50 GPa strongly suggests that the B_2H_6 molecular crystal was experiencing a significant disordering upon compression. However, such disordering may only involve the terminal B–H groups that affect either the crystal lattice or the molecular geometry or both, rather than the bridging B–H groups. This is evidenced by the relatively low pressure dependence of the ν_{17} mode associated with the bridging B–H stretching and ring deformation (Fig. 3), and the fact that the broadening of this mode is much slower than that of the ν_{14} mode (Fig. 4), which is consistent with the strong rigidity of the molecular ring to compression. The initial geometry of the four-member ring with both BHB and HBH angles close to 90° in both the gas phase and low-temperature crystalline phase, seems to change very little even at 50 GPa to maintain this molecular rigidity. Although Barbee III *et al.* proposed a general trend that boranes become unstable at high pressures,[16] our study suggests that diborane is chemically stable up to at least 50 GPa. Further pressure-induced instability may occur in much higher pressure regions. Indeed, decaborane was observed to transform to a nonmolecular phase only at pressures above 100 GPa.[17]

IV. CONCLUSIONS

We investigated pressure-induced structural transformations of diborane up to 50 GPa in a diamond anvil cell using *in situ* synchrotron IR absorption spectroscopy for the first time. The detailed spectroscopic and optical observations allow for the identification of a liquid to solid transition above 3.5 GPa. Further compression results in another two possible transitions around 6.9 and 14.7 GPa. These transitions are evidenced by the reduction in the number of IR bands, the difference in the pressure dependence of the IR frequencies, as well as the bandwidths of representative fundamentals. The solid phases below 14.7 GPa are believed to be ordered crystalline but with possibly different crystal structures. The significant band broadening when compressed to 50 GPa suggests the onset of a disorder of the molecular crystals. Our study shows that the B_2H_6 molecular structure is stable up to 50 GPa while more significant structural changes may occur well beyond 50 GPa.

ACKNOWLEDGMENTS

Y.S. acknowledges the support from a Discovery Grant and a RTI Grant from the NSERC of Canada, a Leaders Opportunity Fund from the Canadian Foundation for Innovation and an Early Researcher Award from the Ontario Ministry of Research and Innovation. C.M. acknowledges the CCP fellowship from UWO. IR measurements were performed at the U2A beamline at the NSLS at BNL. The U2A beamline is supported by COMPRES, the Consortium for Materials Properties Research in Earth Sciences under NSF Cooperative Agreement No. EAR06-49658, U.S. Department of Energy (DOE), (CDAC), and NSF (DMR).

[1] C. L. Yu and S. H. Bauer, J. Phys. Chem. Ref. Data **27**, 807 (1998).
[2] B. M. Mikhailov, Russ. Chem. Rev. **31**, 207 (1962).
[3] W. N. Lipscomb, Pure Appl. Chem. **55**, 1431 (1983).
[4] K. Hedberg and V. Schomaker, J. Am. Chem. Soc. **73**, 1482 (1951).
[5] H. W. Smith and W. N. Lipscomb, J. Chem. Phys. **43**, 1060 (1965).
[6] D. S. Jones and W. N. Lipscomb, J. Chem. Phys. **51**, 3133 (1969).
[7] F. Stitt, J. Chem. Phys. **9**, 780 (1941).
[8] A. N. Webb, J. T. Neu, and K. S. Pitzer, J. Chem. Phys. **17**, 1007 (1949).
[9] R. C. Lord and E. Nielsen, J. Chem. Phys. **19**, 1 (1951).
[10] I. Freund and R. S. Halford, J. Chem. Phys. **43**, 3795 (1965).
[11] J. L. Duncan, D. C. McKean, I. Torto, and G. D. Nivellini, J. Mol. Spectrosc. **85**, 16 (1981).
[12] J. L. Duncan, J. Harper, E. Hamilton, and G. D. Nivellini, J. Mol. Spectrosc. **102**, 416 (1983).
[13] J. F. Stanton, R. J. Bartlett, and W. N. Lipscomb, Chem. Phys. Lett. **138**, 525 (1987).
[14] A. Vijay and D. N. Sathyanarayana, J. Mol. Struct. **351**, 215 (1995).
[15] L. Turker, J. Mol. Struct. **629**, 279 (2003).
[16] T. W. Barbee III, A. K. McMahan, J. E. Klepeis, and M. Van Schilfgaarde, Phys. Rev. B **56**, 5148 (1997).
[17] S. Nakano, R. J. Hemley, E. A. Gregoryanz, A. F. Goncharov, and H. K. Mao, J. Phys.: Condens. Matter **14**, 10453 (2002).
[18] H. K. Mao, J. Xu, and P. M. Bell, J. Geophys. Res. **91**, 4673 (1986).
[19] NIST Chemistry WebBook, http://webbook.nist.gov/chemistry/.